The Sequence, Expression, and Chromosomal Localization of a Novel Polycystic Kidney Disease 1–Like Gene, *PKD1L1*, in Human

Takeshi Yuasa,[1] Bhuvarahamurthy Venugopal,[1] Stanislawa Weremowicz,[2] Cynthia C. Morton,[2,3] Lei Guo,[1] and Jing Zhou[1,*]

[1]*Renal Division, Departments of Medicine,* [2]*Pathology, and* [3]*Obstetrics, Gynecology and Reproductive Biology, Brigham and Women's Hospital and Harvard Medical School, Boston, Massachusetts, 02115, USA*

**To whom correspondence and reprint requests should be addressed. Fax: (617) 525-5861. E-mail: zhou@rics.bwh.harvard.edu.*

Polycystin-1 and polycystin-2 are the products of *PKD1* and *PKD2*, genes that are mutated in most cases of autosomal dominant polycystic kidney disease. Since the first two polycystins were cloned, three new members, polycystin-L, -2L2, and -REJ, have been identified. In this study, we describe a sixth member of the family, polycystin-1L1, encoded by *PKD1L1* in human. The full-length cDNA sequence of *PKD1L1*, determined from human testis cDNA, encodes a 2849-amino-acid protein and 58 exons in a 187-kb genomic region. The deduced amino acid sequence of polycystin-1L1 has significant homology with all known polycystins, but the longest stretches of homology were found with polycystin-1 and -REJ over the 1453- and 932-amino-acid residues, respectively. Polycystin-1L1 is predicted to have two Ig-like PKD, a REJ, a GPS, a LH2/PLAT, a coiled-coil, and 11 putative transmembrane domains. Several rhodopsin-like G-protein-coupled receptor (GPCR) signatures are also found in polycystin-1L1. Dot-blot analysis and RT-PCR revealed that human *PKD1L1* is expressed in testis and in fetal and adult heart. *In situ* hybridization analysis showed that the most abundant and specific expression of *Pkd1l1* was found in Leydig cells, a known source of testosterone production, in mouse testis. We have assigned *PKD1L1* to the short arm of human chromosome 7 in bands p12–p13 and *Pkd1l1* to mouse chromosome 11 in band A2 by fluorescence *in situ* hybridization. We hypothesize a role for polycystin-1L1 in the heart and in the male reproductive system.

INTRODUCTION

Polycystins are a family of transmembrane proteins. Polycystin-1 and -2 are widely expressed [1,2], whereas polycystin-L, -2L2, and -REJ have limited expression [3–6]. Mutations in *PKD1* and *PKD2*, the respective genes encoding polycystin-1 and -2, cause autosomal dominant polycystic kidney disease (ADPKD), one of the most common monogenic diseases (estimated frequency of occurrence, 1 case per 1000 births), characterized by progressive cystic development in the kidney and eventual renal failure [7]. The involvement of other polycystins in disease states is currently unknown. Polycystin-L was the third polycystin isolated, but the first whose function was demonstrated as a Ca^{2+}-regulated, Ca^{2+}-permeable cation channel [8]. Recently, polycystin-2 has also been shown to function similarly as a cation channel, both intracellularly [9] and on cell membranes with [10] or without [11,12] the coexpression of polycystin-1. Advances with regard to polycystin channels have recently been reviewed [13]. Polycystin-2L2 and -REJ are likely to play a role in fertilization because of their specific expression in testis, although additional experimental evidence is required.

Polycystin-1 is a large plasma membrane protein with a number of adhesive domains. Most of its extracellular segment is made up of 16 copies of an 80- to 90-amino-acid immunoglobulin (Ig)-like repeat called the PKD domain [1,14]. One of the PKD domains is situated between a leucine-rich repeat domain and the C-type lectin domain; the rest are arrayed in tandem between an LDL-1A module and an REJ domain. There is a putative GPCR proteolytic site (GPS) and a putative lipid-binding site (LH2/PLAT) between the REJ domain and the first transmembrane region, and in the first intracellular loop, respectively [15,16]. Following a number of transmembrane regions is a

0888-7543/02 $35.00

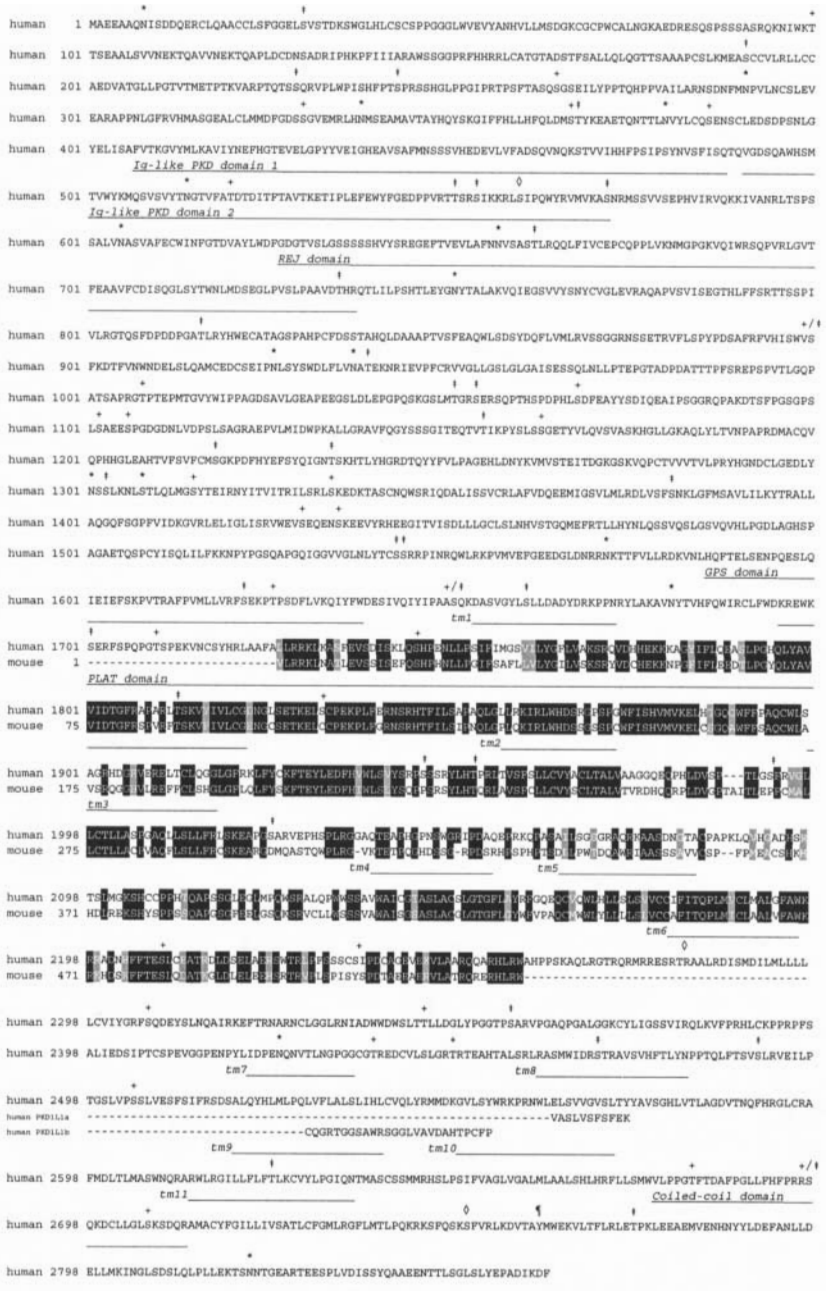

FIG. 1. Deduced amino acid sequences of human polycystin-1L1 and a portion of mouse *Pkd1l1*. ClustalW1.7 and Boxshade 3.21 were used for amino acid sequence alignment. Black and gray shading indicate amino acid identities and similarities, respectively. Various domains are overlined. Potential *N*-glycosylation sites are marked with an asterisk (*). Potential phosphorylation sites are marked as follows: (+) cAMP phosphorylation sites; (◊) protein kinase C phosphorylation sites; (‡) casein kinase phosphorylation sites; (¶) tyrosine kinase phosphorylation sites.

short carboxy-terminal cytoplasmic tail that contains a coiled-coil domain shown to interact *in vitro* with a coiled-coil domain in the C-terminal cytoplasmic region of polycystin-2 [17], and with G-proteins [18] and regulators of G-protein signaling (RGS) proteins [19]. The large size of polycystin-1 has hindered its analysis, and its function remains unknown. Identification of novel proteins closely related to polycystin-1 would not only contribute to a broader understanding of the role of this family of proteins in organ morphogenesis and function, but also would help us to predict the function of polycystin-1 and facilitate our understanding of the pathogenesis of ADPKD.

In this study, we report the identification, chromosomal localization, and expression of a novel gene encoding a

doi:10.1006/geno.2002.6719, available online at http://www.idealibrary.com on IDEAL

TABLE 1: Sequence comparisons between human polycystin-1, -REJ, 1L1, -2, -L, and 2L2

	PC1	PCREJ	**PC1L1**	PC2	PCL	PC2L2
PC1	X	21%	**26%**	32%	33%	28%
	X	38%	**42%**	48%	73%	45%
	X	1371	**856**	150	150	149
PCREJ	20%	X	**22%**	21%	24%	22%
	35%	X	**39%**	39%	41%	41%
	2016	X	**836**	497	395	431
PC1L1	**23%**	**22%**	**X**	**23%**	**21%**	**23%**
	38%	**38%**	**X**	**40%**	**36%**	**39%**
	1453	**932**	**X**	**376**	**536**	**374**
PC2	24%	21%	**26%**	X	52%	48%
	42%	42%	**42%**	X	70%	68%
	425	514	**295**	X	685	579
PCL	25%	25%	**21%**	54%	X	50%
	42%	40%	**40%**	73%	X	68%
	408	253	**490**	685	X	547
PC2L2	24%	22%	**23%**	47%	52%	X
	41%	41%	**40%**	67%	71%	X
	256	497	**355**	606	509	X

Top, middle, and bottom rows indicate the percentage of identity and similarity, and the number of residues of the proteins in the left column that share with the proteins in the top row, respectively. Bold text represents the comparison between PC1L1 and other PCs.

polycystin-1-like protein, polycystin-1L1, in humans. Polycystin-1L1 possesses a topology similar to that of polycystin-1 and contains two Ig-like PKD domains that are followed by a small REJ, a GPS, a LH2/PLAT, a coiled-coil, and 11 putative transmembrane domains.

RESULTS

Isolation and Characterization of cDNAs for a Sixth Polycystin, Polycystin-1L1

Through database searches we identified two genomic sequences of chromosome 7 (EMBL/GenBank acc. nos. AC069282 and AC019066) with similarity to polycystin-2. The deduced amino acid sequence of these clones showed 43% similarity and 25% identity over 282 residues (235–516) with polycystin-2. We tentatively assumed that these genomic sequences encoded a novel polycystin.

We carried out 5′- and 3′-RACE with a human testis cDNA library and obtained a 4.5-kb and a 3-kb fragment. Direct sequencing of the PCR products revealed a 7.3-kb consensus cDNA sequence with an open reading frame, which encodes a protein of 2400 amino acids with termination codons and a consensus polyadenylation signal (5′-AATAAA-3′), but without an ideal initiation codon. We then continued 5′-RACE using the gene-specific primers hP9R4 and AP2 and obtained 2 kb more cDNA. The sequence spanning the first ATG triplet of this cDNA has a G residue at position +4 and a G residue at position –3; this is in complete agreement with the consensus sequence for a mammalian translation initiation site [20].

Thus, this novel cDNA encodes a 2849-amino-acid protein (AB061683; Fig. 1) with homology to all known polycystins (Table 1). Although the sequence homology between this novel polycystin and polycystin-1 or polycystin-REJ is not higher than that with polycystin-2, they share 38% homology over a large region (1453 and 932 amino acids, respectively; Fig. 2A). Phylogenetic analysis of this novel polycystin with the other five known polycystins shows that this novel polycystin belongs to the polycystin-1-like subfamily (Fig. 2B); we thus named it polycystin-1L1.

We determined the exon/intron structure of human *PKD1L1* by comparison of genomic and cDNA sequences (Table 2). In the 187-kb genomic region, we found 58 exons varying in size from 26 bp to 369 bp; the intron size varies from 0.1 kb to 17.0 kb.

Kyte–Doolittle hydropathy analysis of polycystin-1L1 revealed 11 highly hydrophobic regions, suggesting the

A

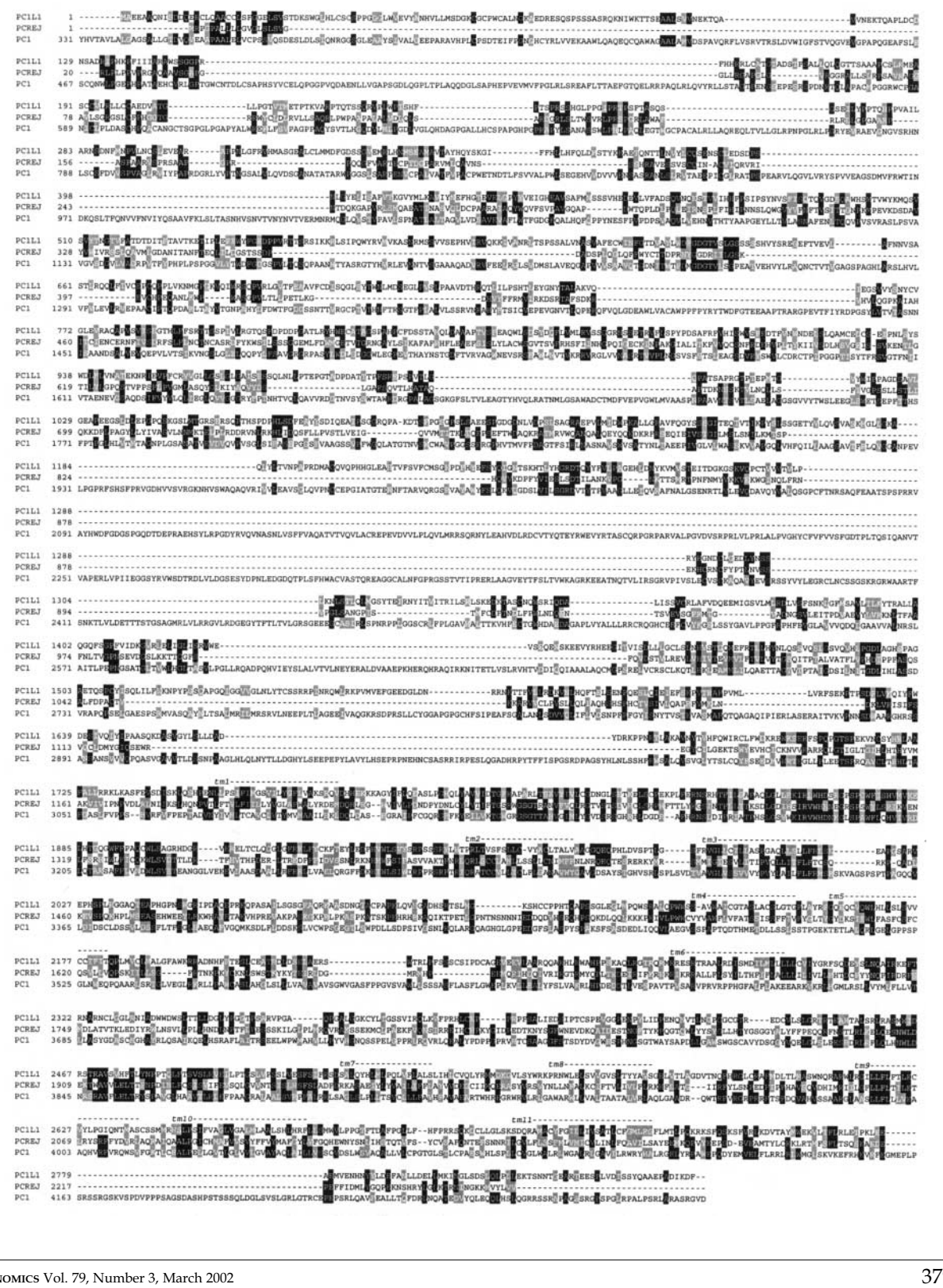

doi:10.1006/geno.2002.6719, available online at http://www.idealibrary.com on IDEAL

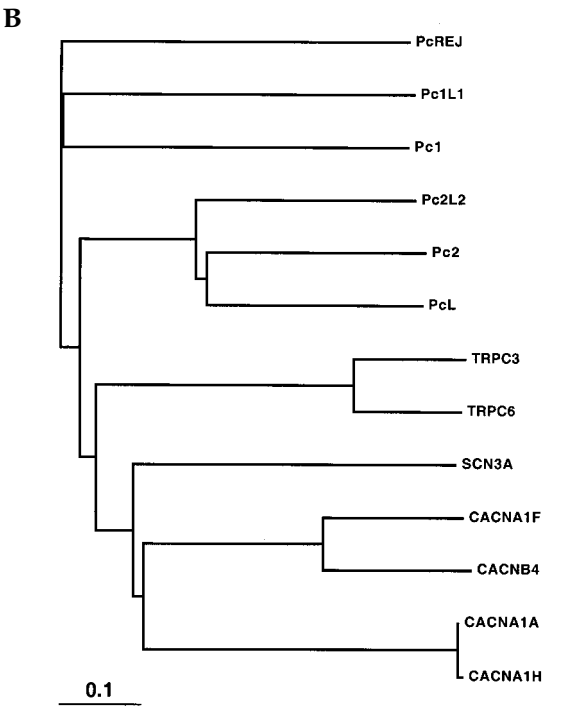

FIG. 2. Protein family classification of polycystin-1L1. (A) (previous page) Comparison among human polycystin-1, polycystin-REJ, and polycystin-1L1. The C-terminal ends of the proteins are indicated by an asterisk. The predicted transmembrane domains are overlined. (B) The deduced phylogenetic relationship among human polycystin-1L1, other polycystins, and homologous proteins. Evolutionary distances (0.1 million years) are shown by the total branch lengths (horizontal lines).

presence of 11 transmembrane segments (Fig. 3A). After further analysis with two more transmembrane prediction programs (TMHMM and TMpred) and comparison of the results with those obtained from the analysis of polycystin-1 and -REJ, we postulated a topology model with 11 transmembrane segments for polycystin-1L1. Analysis with the protein secondary-structure prediction programs SMART and Pfam revealed two Ig-like PKD domains, a small REJ domain, a GPS domain, and an LH2/PLAT domain that are all found in polycystin-1 (Fig. 3B). A coiled-coil structure was predicted in the C-terminal cytoplasmic tail (between residues 2776 and 2811) by the Lupas coiled-coil prediction program (Fig. 3C), as in the other polycystins. The domain structure of polycystin-1L1 also indicates that it is a member of the polycystin-1 subfamily. Notably, polycystin-1L1 has a number of rhodopsin-like GPCR superfamily signatures throughout its sequence.

We identified two smaller bands (2.4 and 2.1 kb) that encode alternatively spliced transcripts of *PKD1L1* during 3′-RACE. Each transcript contained a partial coding sequence and termination codons with a consensus polyadenylation signal (5′-AATAAA-3′) 10 nucleotides upstream from the poly(A) tail. These spliced variants, *PKD1L1a* and *PKD1L1b*, are predicted to contain seven and six transmembrane domains, respectively (Fig. 3D). Although the significance of these alternatively spliced products is unclear, they may provide one way of regulating the abundance of the long transcript.

Determination of Partial cDNA Sequence of Mouse *Pkd1l1*

Through database searches, we identified one genomic sequence (AC024116) of mouse chromosome 11 that is syntenic to human chromosome 7p with similarity to human *PKD1L1*. The DNA sequence of AC024116 showed > 70% identity to human *PKD1L1* (nucleotide sequence from 4956 to 6552 of human *PKD1L1*). We tentatively assumed that this genomic clone contains the mouse ortholog of the *Pkd1l1* gene and designed RT-PCR primers based on the genomic sequence information. We obtained a cDNA fragment of 1594 bp and confirmed it to be the mouse *Pkd1l1* (AB061684) with 72.3% nucleotide identity and 61% and 69% amino acid identity and similarity to its human counterpart, respectively, by DNA sequencing (Fig. 1). This fragment was used as a probe for further northern blot and *in situ* hybridization analysis.

Tissue-Specific Expression of Human and Mouse *PKD1L1* and Their Alternatively Spliced Transcripts

We analyzed the tissue-specific expression of both the human and mouse genes by northern blot analysis using cDNA probes (1.9 kb and 1.6 kb, respectively) amplified by RT-PCR. Neither the human *PKD1L1* nor the mouse *Pkd1l1*, however, was detected by northern blot analysis of multiple tissues (data not shown). We then examined the expression of human *PKD1L1* by dot-blot analysis using the same cDNA probe, and detected *PKD1L1* expression in adult and fetal heart and in testis (Fig. 4A). The expression pattern was further confirmed with RT-PCR from multiple tissues using two sets of primers that can detect all three *PKD1L1* transcripts. Both splicing variants, *PKD1L1a* and *PKD1L1b*, were found in adult testis, but only *PKD1L1a* was found in fetal or adult heart (Fig. 4B). These *PKD1L1* transcripts can be detected by one-round RT-PCR (35 cycles).

Cellular Localization of Mouse *Pkd1l1* by *in Situ* Hybridization

We carried out *in situ* hybridization in various normal mouse tissues, including brain, heart, kidney, and testis, using a 1.6-kb ^{35}S-UTP-labeled *Pkd1l1* antisense riboprobe. Testis showed more widespread expression than did other tissues (Figs. 5A–5D). It is interesting that Leydig cells, which are known to produce testosterone, showed strong expression of *Pkd1l1*. A low level of expression was noticed in seminal ducts, myoid cells, and tunica vaginalis (spindle-shaped cells that surround the basal cell layer of germinal cells and act as a support system). Other tissues, including adrenal gland and heart myocardium, also showed weak

TABLE 2: Exon/intron structure of human *PKD1L1*

exon no.	size (bp)	3′ splice site (acceptor)	5′ splice site (donor)	intron (kb)	interrupted amino acid
1			CTAAG**gt**atc	15.9	
2	103	ttc**ag**AGGAT	GAAAG**gt**gag	4.9	Ar/g
		(initiation site: GAC**ATG**G)			
3	116	ctt**ag**GTGTC	GGTCG**gt**aag	3.0	G/lu
4	125	tct**ag**AGGTC	AGAAG**gt**att	3.3	Lys/Asn
5	113	tac**ag**AACAT	GATAG**gt**atg	1.3	Se/r
6	121	tac**ag**AATTC	TCCAG**gt**tgg	0.6	Gln/Leu
7	218	tta**ag**CTCCA	AGAAG**gt**acg	1.6	Se/r
8	323	cac**ag**CTCCC	AAAAG**gt**aag	13.6	G/ly
9	168	tat**ag**GTATT	CACCA**gt**atg	12.2	L/ys
10	174	tcc**ag**AAGGA	GAAAA**gt**aag	2.8	T/hr
11	120	ttt**ag**GCACT	GCAAT**gt**atg	0.5	S/er
12	169	cac**ag**CCGTC	CAATG**gt**cag	0.5	Tr/p
13	240	tgc**ag**GTATC	AGTAG**gt**gac	2.0	Ar/g
14	133	ccc**ag**GGAAG	TCCAG**gt**agg	4.2	Gln/Ile
15	207	ctt**ag**ATATG	CCAAG**gt**cag	4.0	Lys/Val
16	182	tgc**ag**GTTCA	CTCAG**gt**gag	3.0	Ar/g
17	222	aac**ag**GTATC	TTCAG**gt**acc	2.4	Ar/g
18	161	ttc**ag**ATTCG	AGAAG**gt**aaa	1.9	V/al
19	369	tta**ag**TTCCC	CTCTG**gt**aag	1.0	A/sp
20	60	tat**ag**ATTTT	GCCAG**gt**gac	2.6	A/la
21	177	cct**ag**CTAAG	CTCAG**gt**atg	0.9	G/ly
22	78	tgc**ag**GTATT	TGTGG**gt**atg	3.0	A/la
23	143	ttt**ag**CTTCG	AACCG**gt**acg	1.3	Pro/Asp
24	121	cat**ag**GACTT	CAAAG**gt**aag	2.0	V/al
25	112	cac**ag**TCATG	GACCT**gt**gag	7.3	Le/u
26	196	ttc**ag**GTATA	ATCAG**gt**atg	1.1	Gln/Glu
27	57	gtc**ag**GAAGA	ATAAG**gt**aag	6.8	Leu/Gly
28	213	tgc**ag**CTAGG	TGTTG**gt**aag	1.0	Gln/Ile
29	228	ttc**ag**GGTTG	GGCAG**gt**aca	2.3	Leu/Asp
30	111	cca**ag**ATTGG	GCCTG**gt**aag	0.1	Ar/g
31	158	gac**ag**GATAA	GTAAG**gt**gtg	1.7	A/sp
32	101	cct**ag**ATTCT	GAAAG**gt**cag	5.9	Val/His
33	193	ttt**ag**ATGCC	TGCAG**gt**ata	1.8	Se/r
34	84	cct**ag**CTACC	CAGAG**gt**aag	1.8	Se/r
35	208	tat**ag**CCACC	CAAAG**gt**agc	2.4	Lys/Val
36	107	ttg**ag**GTGTA	CTGAG**gt**att	0.8	Se/r
37	217	tcc**ag**CGCTC	GGAAG**gt**agg	2.3	Lys/Leu
38	174	ttc**ag**CTTTT	AGCAG**gt**gag	1.7	Gln/Pro
39	111	tgc**ag**CCCCA	GCAAG**gt**acc	0.2	Lys/Gln
40	73	tgc**ag**GAAGC	CCATG**gt**aaa	0.6	G/ly
41	47	atc**ag**GTCCT	GCAAG**gt**aaa	1.1	Lys/Gln
42	163	tct**ag**CAACC	TCAAG**gt**aac	1.8	A/la
43	136	cgc**ag**CACCC	TACAG**gt**gag	1.1	Ar/g
44	85	ggc**ag**GTTTG	TTATG**gt**aag	0.4	Cy/s
45	177	tcc**ag**GTATG	AAAAA**gt**aaa	2.0	Lys/Val
46	119	gac**ag**GTCTT	CTGAG**gt**ggg	6.2	Ar/g
47	111	tac**ag**AGACA	ACAAG**gt**agg	5.6	Ar/g
48	124	tta**ag**AAATG	CTCAG**gt**gag	1.3	Gln/Pro
49	84	ttc**ag**CCTGG	GCAAG**gt**aag	0.6	Lys/Pro
50	173	tgc**ag**CCTCC	ACAAG**gt**cag	1.0	Ar/g
51	235	tac**ag**GACTG	CCCAG**gt**gag	2.2	Gln/Leu
52	105	acc**ag**CTGGT	TGGAG**gt**agc	1.9	Glu/Leu
53	141	tcc**ag**CTCTC	ATCAG**gt**aca	4.9	Gln/Arg
54	135	ctc**ag**AGGGC	CAGGG**gt**aag	2.3	Gly/Gln
55	231	tgc**ag**CTGGT	GAATG**gt**aag	4.5	Met/Leu
56	162	cct**ag**CTGAG	ATCAC**gt**aag	3.2	His/Asn
57	171	ttc**ag**AATTA	CTGAG**gt**aag	5.2	Glu/Pro
58			termination site:		
	26	ttt**ag**CCAGC	GACTTC**TGA**		

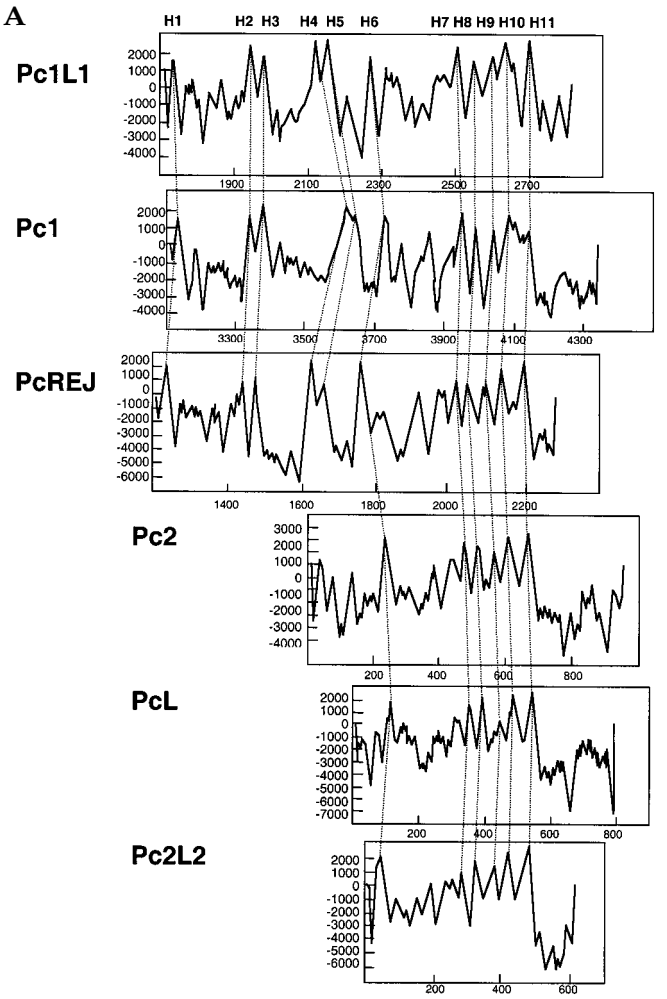

FIG. 3. Peptide sequence analysis and alternative splicing of PKD1L1. (A) Hydropathy analysis of human polycystin family. Hydrophobic peaks are indicated as H1-H11. (B) (opposite page) Alignment analysis of PKD, GPS, and LH2/PLAT domains. The following key represents consensus amino acid residues or respective amino acid classes: (o) alcohol; (l) aliphatic; (.) any; (a) aromatic; (c) charged; (h) hydrophobic; (–) negative; (p) polar; (+) positive; (s) small; (u) tiny; (t) turnlike. (C) (opposite page) Predicted coiled-coil domain of polycystin-1L1. (D) (opposite page) Schematic representation of the splicing variants. Boxes indicate exons. Solid lines indicate introns.

expression for *Pkd1l1*. In addition, we have localized *PKD1L1* to human chromosome 7p12–p13 and *Pkd1l1* to mouse chromosome 11 in band A2 by FISH (data not shown).

Discussion

Polycystin-1L1 has two Ig-like PKD domains, a small REJ domain, a GPS domain in the N-terminal extracellular region, a LH2/PLAT domain in the first intracellular loop, and 11 transmembrane domains. The Ig-like PKD domains of polycystin-1 mediate specific homophilic interactions *in vitro* and are involved directly in the cellular adhesive process in culture [21]. Application of an anti-PKD domain antibody to cultured MDCK cells perturbs their normal epithelial architecture. These results suggest that the PKD domains of polycystin-1L1 play important roles for cell adhesion and signal transduction through homophilic or heterophilic interactions mediated by these domains. By contrast to the REJ domains of polycystin-1 and -REJ (525 and 544 residues, respectively), the REJ domain in polycystin-1L1 is smaller, with only 111 amino acids (between residues 726 and 836). This domain is believed to be associated with calcium transport during fertilization in sea urchins [22].

The GPS domain in polycystin-1L1 is homologous to those in members of the GPCR subfamily, which includes the calcium-independent latrotoxin receptor (CL-1/latrophilin) and flamingo, a newly identified protein of the cadherin superfamily [15,23,24]. The GPS domains of several such genes are shown in Fig. 3B. Lectomedin is a human homolog of CIRL/latrophilin; cadherin, EGF LAG seven-pass G-type receptor is a seven-transmembrane protein first described in *Drosophila*, where it was found in cell/cell boundaries and was believed to play specific roles in protein–protein interactions [24]. All the above evidence supports our hypothesis that polycystin-1L1 has several important functions in protein–protein and/or cell–cell interactions. It is interesting to note that one form of *PKD1L1*, *PKD1L1a*, has seven transmembrane domains like most GPCRs, and also has a number of rhodopsin-like GPCR motifs in its sequence, indicating that polycystin-1L1 or one of its isoforms functions as a GPCR. Indeed, two interesting studies have linked the C-terminal cytoplasmic domain of polycystin-1 with G-protein-coupled signaling pathways by direct binding and activating of G-protein [18], and by directly binding to RGS proteins and terminating this signaling pathway [19]. Very recently, it has been shown that polycystin-1 acts as a G-protein coupled receptor [34].

The LH2/PLAT domain of polycystin-1L1 contains a β-barrel LH2 domain homologous to a noncatalytic domain of lipoxygenases. This domain in lipoprotein lipase is proposed to possess a lipid-binding function and may have an internal conserved ligand-binding site [16,25]. Many lipoprotein lipase family proteins possess the LH2/PLAT

B PKD domain

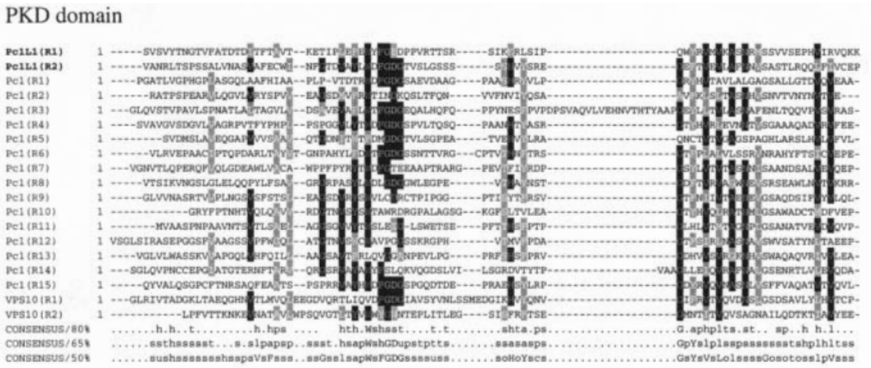

GPS domain

Genbank accession numbers for genes mentioned to the left:

Gene name	Accession number
human homologue to yeast vacuolar protein-sorting 10 protein (VPS10)	AL133395
human lectomedin 1α	AF104266
human lectomedin 1β	AF104938
human lectomedin 1γ	AL157903
human lectomedin 2	AF307079
human lectomedin 3	AF307080
human EGF-TM7 subfamily protein with a large extracellular domain (ETL)	AF192403
CD97	U76764
human EGF-like module-containing mucin-like receptor 2 (EMR2)	AF114491
hEMR3	AF239764
cadherin, EGF LAG seven-pass G-type receptor 1 (CELS1)	AF231024
CELS2	AF234887
human arachidonate 12-lipoxygenase (ALOX12B)	D12638
human arachidonate lipoxygenase-3 (ALOXE3)	AJ269499
human pancreatic lipase (PNLIP)	J05125
human pancreatic lipase related protein 1 (PNLIPRP1)	M93283
PNLIPRP2	M93284
human endothelial lipase (LIPG)	AF118767
human hepatic lipase (LIPC)	J03895

LH2/PLAT domain

C

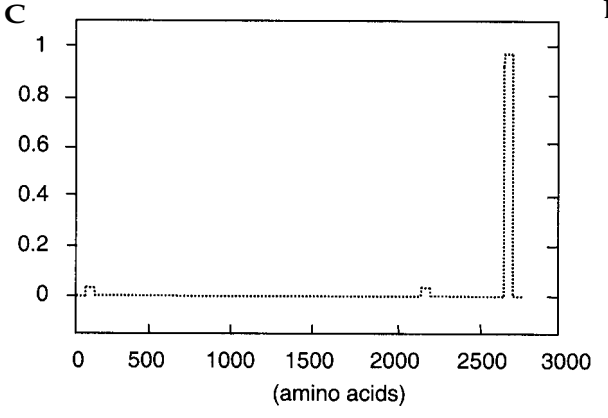

D

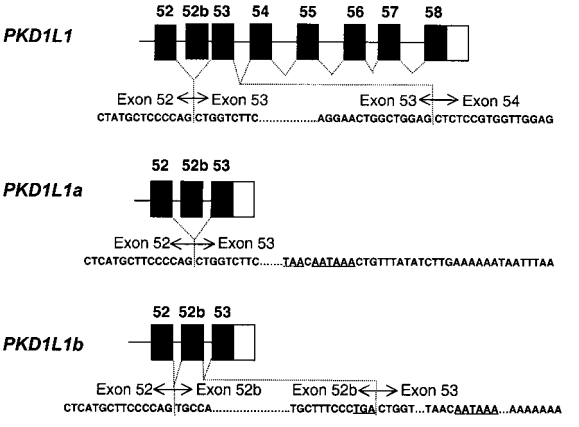

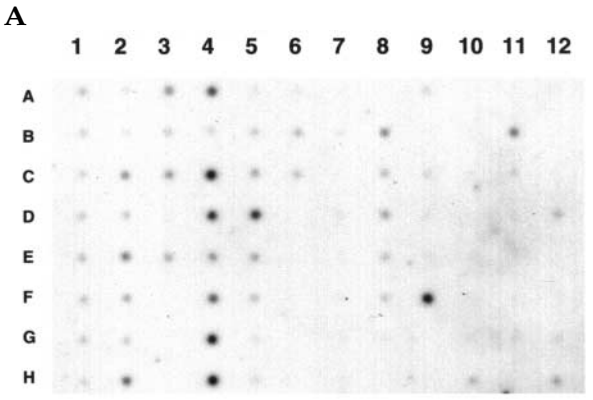

	1	2	3	4	5	6	7	8	9	10	11	12
A	whole brain	cerebellum, left	substantia nigra	heart	esophagus	colon, transverse	kidney	lung	liver	leukemia, HL-60	fetal brain	yeast total RNA
B	cerebral cortex	cerebellum, right	accumbens nucleus	aorta	stomach	colon, desending	skeletal muscle	placenta	pancreas	HeLa S3	fetal heart	yeast tRNA
C	frontal lobe	corpus callosum	thalamus	atrium, left	duodenum	rectum	spleen	bladder	adrenal gland	leukemia, K-562	fetal kidney	*E. coli* rRNA
D	parietal lobe	amygdala	pituitary gland	atrium, right	jejunum		thymus	uterus	thyroid gland	leukemia, MOLT-4	fetal liver	*E. coli* DNA
E	occipital lobe	caudate nucleus	spinal cord	ventricle, left	ileum		peripheral blood leukocyte	prostate	salivary gland	Burkitt's lymphoma, Raji	fetal spleen	Poly r(A)
F	temporal lobe	hippo-campus		ventricle, right	ilocecum		lymph node	testis	mammary gland	Burkitt's lymphoma, Daudi	fetal thymus	human Cot-1 DNA
G	p. c.* of cerebral cortex	medulla oblongata		inter-ventricular septum	appendix		bone morrow	ovary		colorectal adeno-carcinoma, SW480	fetal lung	human DNA 100 ng
H	pons	putamen		apex of the heart	colon, ascending		trachea			lung carcinoma, A549		human DNA 500 ng

* paracentral gyrus

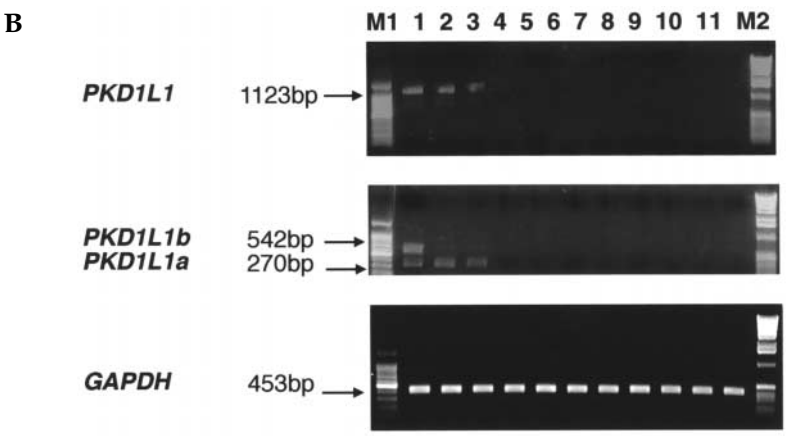

FIG. 4. Expression of *PKD1L1*. (A) Human RNA dot-blot analysis using the C-terminal 1.9 kb of coding sequence as a probe. (B) RT-PCR analysis of human fetal and adult tissues. Top row indicates RT-PCR amplified by *PKD1L1* specific 3′ primer pair A. Middle row indicates RT-PCR amplified by *PKD1L1*-specific 3′ primer pair B. The expression of *GAPDH* is used as a positive control for the RNA (bottom row). Lanes M1, 100-bp ladder; 1, adult testis; 2, adult heart; 3, fetal heart; 4, adult kidney; 5, fetal kidney; 6, fetal brain; 7, fetal cerebellum; 8, fetal lung; 9, fetal muscle; 10, fetal eye; 11, fetal liver; M2, 1-kb ladder.

domain (Fig. 3B). When we consider that the lipoprotein metabolism plays an important role in the male reproductive system, it is interesting to note the relatively high levels of *Pkd1l1* expression in testis and that *lov1*, a *Caenorhabditis elegans* homolog of *PKD* genes, is required for male mating behavior in these worms [26]. Polycystin-1L1 has a short C-terminal cytoplasmic tail with a coiled-coil domain that is also found in polycystin-1 and is believed to be the domain interacting with a coiled-coil domain in the C-terminal cytoplasmic region of polycystin-2 [16]. Polycystin-1L1 also has strong motif sequences for putative phosphorylation sites in the C-terminal cytoplasmic region: one for protein kinase C, one for casein kinase, and one for tyrosine kinase. Phosphorylation of these motif sequences may be involved in the regulation of downstream signaling mediated by polycystin-1L1.

Our FISH analyses have assigned *PKD1L1* to chromosome 7p12–p13 in humans and *Pkd1l1* to mouse chromosome 11 in band A2, which is linked to the mouse mutation *jck*, a naturally occurring mouse line with recessive polycystic kidney disease [27]. However, it is unlikely that *Pkd1l1* is the gene for polycystic kidney disease in these mice, as we could not detect any expression of *Pkd1l1* in mouse kidney. The specific, albeit low, levels of *PKD1L1* expression in human fetal and adult heart raise the possibility of its involvement in heart diseases. Indeed, gene targeting experiments have recently shown that homozygous mice with mutations in *Pkd1* develop not only kidney, pancreas, and skeletal defects but also cardiovascular abnormalities [28–30].

Materials and Methods

Isolation of human PKD1L1 and mouse Pkd1l1. We used primers specific to the putative exonic sequence in genomic clone RP11-61L9 (AC069282) to carry out 5′- and 3′-RACE on human testis Marathon-Ready cDNA (Clontech, Palo Alto, CA). AdvanTaq DNA polymerase (Clontech) was used to perform touchdown PCR with cycling parameters as follows: initial denaturation of 94°C for 2 minutes; 5 cycles of 94°C for 30 seconds, 72°C for 4 minutes; 5 cycles of 94°C for 30 seconds, 70°C for 4 minutes; 25 cycles of 94°C for 30 seconds, 68°C for 4 minutes, and a final extension at 68°C for 7 minutes, as described [5]. The primer sequences used in this study are listed in Table 3. For 5′-RACE, primers AP1 (Clontech) and hP9R1 were used to do the first PCR. Nested PCR was carried out using 1 μl of the diluted first PCR product (1:100) and the nested primers AP2 (Clontech) and hP9R2. For the second 5′-RACE, primers AP1 and hP9R3, and nested primers AP2 and hP9R4 were used. 3′-RACE was carried out similarly with primers AP1 and hP9F1, and nested primers AP2 and hP9F2. Prominent bands were excised from the agarose gel, purified, and sequenced.

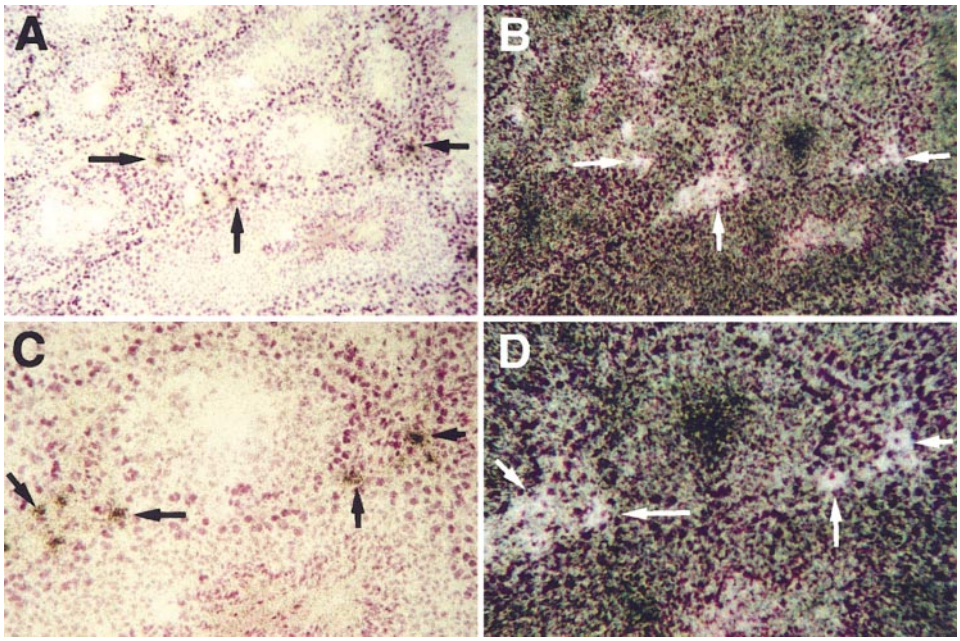

FIG. 5. Localization of *Pkd1l1* expression in mice testis by RNA *in situ* hybridization. Bright- (A, C) and dark-field (B, D) photographs show the *Pkd1l1* expression. Arrows indicate sites of *Pkd1l1* expression. (B) and (D) Single seminiferous tubule and its surrounding Leydig cells, showing strong expression of *Pkd1l1*. Magnification: (A, B) ×100; (C, D) ×200.

The sequences obtained were compared with the sequences of the clones RP11-61L9 and RP11-164L4 (AC019066).

Primers specific to the putative exonic sequence in mouse genomic clone RP23-298M16 (mP9F1 and mP9R1) were used to perform RT-PCR on mouse testis cDNA similarly as described above.

Sequence analysis. We aligned DNA sequences obtained by 5′-RACE and 3′-RACE to get an overall consensus sequence. Alignment analysis was performed with ClustalW (http://clustalw.genome.ad.jp/) and Boxshade3.21 (http://www.ch.embnet.org/software/BOX_form.html). The programs MOTIF (http://motif.genome.ad.jp/), SMART (Simple Modular Architecture Research Tool) (http://smart.embl-heidelberg.de/), and Pfam (Protein families database) (http://www.sanger.ac.uk/Software/Pfam/search.shtml) were used to predict protein function and localization. The programs TMHMM (http://genome.cbs.dtu.dk/services/TMHMM/) and TMpred (Prediction of Transmembrane Regions and Orientation) (http://www.ch.embnet.org/software/TMPRED_form.html) were used to predict the transmembrane helices. Prediction of coiled-coil structure by Lupas algorithm was performed with Coils (http://www.ch.embnet.org/software/COILS_form.html) [31]. The phylogenetic trees were plotted using Treeview [32].

TABLE 3: Primer sequences used in this study

name	sequence	position (exon: nucleotides)
human *PKD1L1*		
hP9F1	GAATTTTCCAAACCTGTTACAAGGGC	31: 4810-4836
hP9F2	CACGGGACAGGGCTGGTTCTTCCCTGC	37: 5656-5684
hP9F3	CCCGACTCAGGGCCAGCATGTGGATTG	51: 7370-7395
hP9R1	GAGGGGACGAGACTCCCCGTAGGGAGGA	51: 7484-7631
hP9R2	CGGCGTGTGCAGGTAGCGGCTGGAGGA	38: 5839-5864
hP9R3	TCACTCCCAGCCTCACAGGCTGAGACCTCC	15: 2069-2098
hP9R4	CTGGCATTTACCAGAGCTGAGGAGGGGGA	13: 1792-1820
hP9R5	GACTCTCTTCTGTCCTTGCCTCCCCTGTGT	57: 8462-8491
human *PKD1L1a*		
hP9R6	TTTTTCAAAAGAAAATGACACAAGAGAGGCT	52: 7615-7639
mouse *Pkd1l1*		
mP9F1	TGTCCTAAGAAGAAAGCTGAATGCCA	3572-3600
mP9R1	CCAGCGCAGGTGGCGTTCTCGTTGTCGG	3703-3730
human *GAPDH*		
GAPDH/F	GACCACAGTCCATGCCATCACT	8: 525-546
GAPDH/R	TCCACCACCCTGTTGCTGTAG	9: 957-977
adapter primers (CLONTECH)		
AP1	CCATCCTAATACGACTCACTATAGGGC	
AP2	ACTCACTATAGGGCTCGAGCGGC	

RNA dot blot, northern blot hybridization, and RT-PCR. We hybridized human Multiple Tissue Array (Clontech) and Multiple Tissue Northern Blot (Clontech) with a randomly labeled 1.9-kb coding sequence of *PKD1L1* (nucleotide sequence 5658–7511) amplified by RT-PCR using hP9F2 and hP9R1, in ExpressHyb Hybridization Solution (Clontech) at 65°C and 50°C overnight, respectively, as described [5]. Mouse Multiple Tissue Northern Blot (Clontech) was hybridized with a randomly labeled 1.5-kb coding cDNA probe of mouse *Pkd1l1* (mP9F1-mP9R1) in ExpressHyb Hybridization Solution (Clontech) at 50°C overnight. The radiolabeled membranes were washed twice in 2× SSC, 0.05% SDS at 50°C and twice in 0.1× SSC, 0.1% SDS at 50°C. Signals were visualized by autoradiography.

Total cellular RNA of human adult and fetal tissues for RT-PCR was prepared as described [5], and first-strand cDNA was synthesized from 5 mg of total RNA using Superscript II (GIBCO, Gaithersburg, MD). Two primer sets (hP9F3-hP9R5 and hP9F3-hP9R6) were synthesized according to the nucleotide sequence of human *PKD1L1* or *PKD1L1a*, respectively. Human glyceraldehyde-3-phosphate dehydrogenase (*GAPDH*) gene-specific primers, GAPDH/F and GAPDH/R were used as controls. Portions (1 μl) of the cDNA were amplified by PCR with cycling parameters as follows: 94°C for 30 seconds, 60°C for 30 seconds, 72°C for 1 minute, with 35 cycles for *PKD1L1* and 25 cycles for *GAPDH* [5].

In situ hybridization. We carried out *in situ* hybridization of mouse *Pkd1l1* gene as described [33]. The following materials were obtained from the indicated sources: T7 RNA polymerase, RNasin, and DNase I (Promega, Madison, WI); dithiothreitol (DTT), formamide, and restriction endonuclease (Roche Molecular Biochemicals, Indianapolis, IN). The 1.6-kb RT-PCR fragment of mouse *Pkd1l1* (mP9F1-mP9R1) was cloned into Bluescript SK vector (Stratagene, La Jolla, CA), which was linearized with *Xba*I for sense and *Xho*I for antisense riboprobe preparation using T7 and T3 promoter, respectively. Transcription was carried out essentially as recommended by the manufacturer with 200–600 ng of linearized DNA as template. ^{35}S-UTP (DuPont NEN, Boston, MA)-labeled sense and antisense riboprobe (5×10^4 cpm) was hydrolyzed in 0.1 M DTT to an average size of 100 bases, and hybridization was carried out at 55°C overnight. The slides were then washed in 5× SSC containing 10 mM DTT at 55°C for 30 minutes, and in 2× SSC containing 50% formamide and 10 mM DTT at 65°C for 30 minutes. Finally, the slides were dipped in NTB-2 autoradiographic emulsion (Eastman Kodak, Rochester, NY) and stored in complete darkness at 4°C for 2 weeks. The slides were developed with Kodak D-19 developer (Eastman Kodak) and counterstained with hematoxylin/eosin. The experiment was repeated once to validate expression and localization. Control sense RNA probes were used to verify the specificity of the signal.

Acknowledgments

We thank C. Stayner, M. Lakkis, and H. Tsukaguchi for constructive discussion, and E. Williams for technical assistance (Brigham and Women's Hospital and Harvard Medical School). This work was supported in part by the Uehara Memorial Foundation Research Fellowship to T. Y. and the grants from the National Institute of Diabetes, Digestive and Kidney Diseases (NIDDK) to J.Z.

RECEIVED FOR PUBLICATION SEPTEMBER 7;
ACCEPTED DECEMBER 27, 2001.

References

1. The International Polycystic Kidney Disease Consortium. (1995). Polycystic kidney disease: the complete structure of the *PKD1* gene and its protein. *Cell* **81:** 289–298.
2. Schneider, M. C., *et al.* (1996). A gene similar to *PKD1* maps to chromosome 4q22: a candidate gene for *PKD2*. *Genomics* **38:** 1–4.
3. Nomura, H., *et al.* (1998). Identification of *PKDL*, a novel polycystic kidney disease 2-like gene whose murine homologue is deleted in mice with kidney and retinal defects. *J. Biol. Chem.* **273:** 25967–25973.
4. Veldhuisen, B., Spruit, L., Dauwerse, H. G., Breuning, M. H., and Peters, D. J. (1999). Genes homologous to the autosomal dominant polycystic kidney disease genes (*PKD1* and *PKD2*). *Eur. J. Hum. Genet.* **7:** 860–872.
5. Guo, L., *et al.* (2000). Identification and characterization of a novel polycystin family member, polycystin-L2, in mouse and human: sequence, expression, alternative splicing, and chromosomal localization. *Genomics* **64:** 241–251.
6. Hughes, J., Ward, C. J., Aspinwall, R., Butler, R., and Harris, P. C. (1999). Identification of a human homologue of the sea urchin receptor for egg jelly: a polycystic kidney disease-like protein. *Hum. Mol. Genet.* **8:** 543–549.
7. Calvet, J. P., and Grantham, J. J. (2001). The genetics and physiology of polycystic kidney disease. *Semin. Nephrol.* **21:** 107–123.
8. Chen, X. Z., *et al.* (1999). Polycystin-L is a calcium-regulated cation channel permeable to calcium ions. *Nature* **401:** 383–386.
9. Vassilev, P. M., *et al.* (2001). Polycystin-2 is a novel cation channel implicated in defective intracellular Ca^{2+} homeostasis in polycystic kidney disease. *Biochem. Biophys. Res. Commun.* **282:** 341–350.
10. Hanaoka, K., *et al.* (2000). Co-assembly of polycystin-1 and -2 produces unique cation-permeable currents. *Nature* **408:** 990–994.
11. Gonzalez-Perrett, S., *et al.* (2000). Polycystin-2, the protein mutated in autosomal dominant polycystic kidney disease (ADPKD), is a Ca^{2+}-permeable nonselective cation channel. *Proc. Natl. Acad. Sci. USA* **96:** 6371–6376.
12. Chen, X. Z., *et al.* (2001). Transport function of the naturally occurring pathogenic polycystin-2 mutant, R742X. *Biochem. Biophys. Res. Commun.* **282:** 1251–1256.
13. Stayner, C., and Zhou, J. (2001). Polycystin channels and kidney disease. *Trends Pharmacol. Sci.* **22:** 543–546.
14. Hughes, J., *et al.* (1995). The polycystic kidney disease 1 (*PKD1*) gene encodes a novel protein with multiple cell recognition domains. *Nat. Genet.* **10,** 151–160.
15. Ponting, C. P., Hofmann, K., and Bork, P. (1999). A latrophilin/CL-1-like GPS domain in polycystin-1. *Curr. Biol.* **9:** R585–R588.
16. Bateman, A., and Sandford, R. (1999). The PLAT domain: a new piece in the *PKD1* puzzle. *Curr. Biol.* **9:** R588–R590.
17. Qian, F., *et al.* (1997). *PKD1* interacts with *PKD2* through a probable coiled-coil domain. *Nat. Genet.* **16:** 179–183.
18. Parnell, S. C., *et al.* (1998). The polycystic kidney disease-1 protein, polycystin-1, binds and activates heterotrimeric G-proteins *in vitro*. *Biochem. Biophys. Res. Commun.* **251:** 625–631.
19. Kim, E., *et al.* (1999). Interaction between RGS7 and polycystin. *Proc. Natl. Acad. Sci. USA* **96:** 6371–6376.
20. Kozak, M. (1996). Interpreting cDNA sequences: some insights from studies on translation. *Mamm. Genome* **7:** 563–574.
21. Ibraghimov-Beskrovnaya, O., *et al.* (2000). Strong homophilic interactions of the Ig-like domains of polycystin-1, the protein product of an autosomal dominant polycystic kidney disease gene, *PKD1*. *Hum. Mol. Genet.* **9:** 1641–1649.
22. Moy G. W., *et al.* (1996). The sea urchin sperm receptor for egg jelly is a modular protein with extensive homology to the human polycystic kidney disease protein, *PKD1*. *J. Cell Biol.* **33:** 809–817.
23. Geppert, M., *et al.* (1998). Neurexin I (is a major (-latrotoxin receptor that cooperates in (-latrotoxin action. *J. Biol. Chem.* **273:** 1705–1710.
24. Usui, T., *et al.* (1999). Flamingo, a seven-pass transmembrane cadherin, regulates planar cell polarity under the control of Frizzled. *Cell* **98:** 585–595.
25. Nielsen, M. S., *et al.* (1997). Segments in the C-terminal folding domain of lipoprotein lipase important for binding to the low density lipoprotein receptor-related protein and to heparan sulfate proteoglycans. *J. Biol. Chem.* **272:** 5821–5827.
26. Barr, M. M., and Sternberg, P. W. (1999). A polycystic kidney-disease gene homologue required for male mating behaviour in *C. elegans*. *Nature* **401:** 386–389.
27. Atala, A., Freeman, M. R., Mandell, J., and Beier, D. R. (1993). Juvenile cystic kidneys (*jck*): a new mouse mutation which causes polycystic kidneys. *Kidney Int.* **43:** 1081–1085.
28. Lu, W., *et al.* (1997). Perinatal lethality with kidney and pancreas defects in mice with a targetted *Pkd1* mutation. *Nat. Genet.* **17:** 179–181.
29. Lu, W., *et al.* (1999). Late onset of renal and hepatic cysts in *Pkd1*-targeted heterozygotes. *Nat. Genet.* **21:** 160–161.
30. Boulter, C., *et al.* (2001). Cardiovascular, skeletal, and renal defects in mice with a targeted disruption of the *Pkd1* gene. *Proc. Natl. Acad. Sci. USA* **98:** 12174–12179.
31. Lupas, A., Van Dyke, M., and Stock, J. (1991). Predicting coiled coils from protein sequences. *Science* **252:** 1162–1164.
32. Page, R. D. (1996). TreeView: an application to display phylogenetic trees on personal computers. *Comput. Appl. Biosci.* **12:** 357–358.
33. Venugopal, B., Sharon, R., Abramovitz, R., Khasin, A., and Miskin, R. (2001). Plasminogen activator inhibitor-1 in cardiovascular cells: rapid induction after injecting mice with kainate or adrenergic agents. *Cardiovasc. Res.* **49:** 476–483.
34. Delmas, P., *et al.* Constitutive activation of G-proteins by polycystin-1 is antagonized by polycystin-2. *J. Biol. Chem.* (in press).

Sequence data from this article have been deposited with the DDBJ/EMBL/GenBank Data Libraries under accession numbers AB061683 and AB061684.